Huang *et al.*
Cell Communication and Signaling (2025) 23:107
https://doi.org/10.1186/s12964-025-02060-y

Cell Communication and Signaling

RESEARCH

Open Access

Targeting A2M-LRP1 reverses uterine spiral artery remodeling disorder and alleviates the progression of preeclampsia

Zhengrui Huang[1†], Ping Zhang[6†], Ruiping Chen[1†], Lu Sun[1], Jingyun Wang[5], Ruiling Yan[2], Mengyuan Liu[2], Yuzhen Ding[7], Jian Wang[1], Jiachun Wei[1], Wanchang Yin[1], Xinyao Lu[1], Guang Wang[3*], Xuesong Yang[3,4*] and Ruiman Li[1*]

Abstract

Background Patients with early-onset preeclampsia (EOPE) have a most severe disease state. a2-macroglobulin (A2M) play a crucial role in the pathogenesis of EOPE, but its molecular basis and therapeutic potential remain unclear. This study aimed to elucidate the mechanisms of A2M in EOPE progression and explore the potential of A2M in the treatment of EOPE.

Methods A2M-Low Density Lipoprotein Receptor-Related Protein 1 (LRP1) blocker Receptor-associated protein (RAP) were utilized to alleviate the disease symptom of lipopolysaccharide (LPS) induced preeclampsia rat model. RNA-seq data sourced from public databases and morphological experiments were utilized to examine the relationship between the main fate of smooth muscle cell (SMC) during uterine spiral artery remodeling (SPA-REM) and A2M. Proteomic sequencing analysis of A2M overexpression rat placenta was used to identify the underlying mechanism. Further, LC-MS/MS analysis combined with Co-immunoprecipitation (Co-IP) was used to examine the interacting between A2M and underlying mechanism.

Results Single-cell analysis and morphological experimental results suggest that SMC phenotype switching disorder is the main fate of SMC in the pathological of SPA-REM disorder, and A2M has a causal relationship with this process. Proteomic sequencing data suggest that A2M participates in this process through the RhoA-GTPase pathway, further experimental data provide evidences that A2M can directly upregulate RhoA-GTPase. Cytological and explant experiments suggest that RAP has better efficacy than A2M knockdown AAV vector, finally the efficacy of RAP was verified in the rat model of preeclampsia.

Conclusion SMC A2M promotes the progression of preeclampsia by directly upregulating RhoA-GTPase. Our findings also reveal that A2M serve as a potential target for EOPE and provide a preliminary therapy for inhibit the combination of A2M-LRP1.

†Zhengrui Huang, Ping Zhang and Ruiping Chen contributed equally to this work.

*Correspondence:
Guang Wang
t_wangguang@jnu.edu.cn
Xuesong Yang
yangxuesong@jnu.edu.cn
Ruiman Li
ruimanli@jnu.edu.cn
Full list of author information is available at the end of the article

Keywords Preeclampsia, A2-macroglobulin, Smooth muscle cells, Uterine spiral artery, Phenotype switching

Graphical Abstract

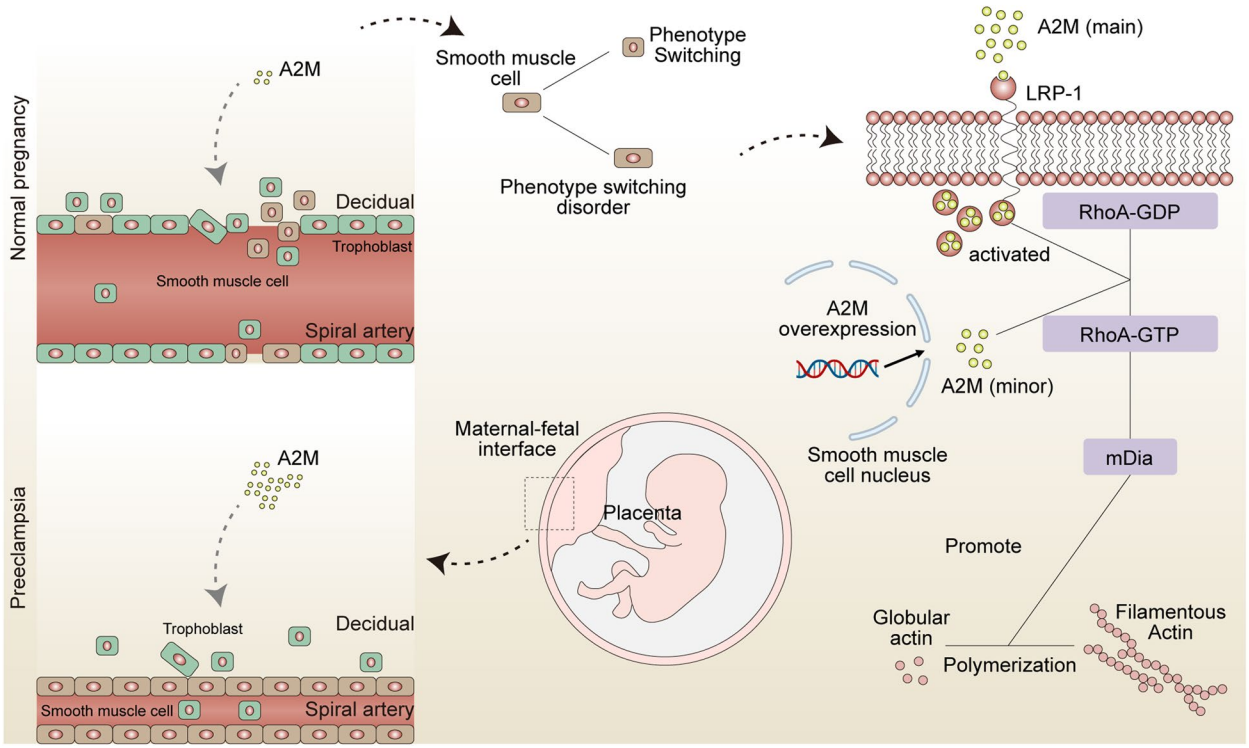

Introduction

Preeclampsia (PE), one severe manifestation of hypertensive disorders of pregnancy, are endangering 2–4% of pregnant women during the perinatal period, PE manifests through distinct pathological mechanisms depending on the timing of its onset. Early-onset preeclampsia (EOPE), occurring before 34 weeks of gestation, is primarily associated with placental abnormalities arising from various causes. In contrast, late-onset preeclampsia (LOPE), which occurs after 34 weeks of gestation, is predominantly linked to maternal metabolic disorders or cardiovascular system abnormalities, with placental function typically remaining relatively normal [1, 2]. Recent advancements have identified various therapeutic targets, and the most promising is targeted delivery therapy of Fms Related Receptor Tyrosine Kinase 1 (FLT-1) knockdown using nanoparticles combined with small Interfering RNA (siRNA) technology [3]. Additionally, targets, such as programmed Death-1 (PD-1) / Programmed Death-Ligand 1 (PD-L1) [4, 5] and T-cell Immunoglobulin and Mucin Domain-Containing Protein 3 (Tim-3) [6], have also garnered interest. Therefore, exploring new therapeutic targets will provide novel insights into PE treatment.

As a secreted protein primarily produced by the liver, macrophages, and NK cells [7, 8], A2M, has received interest for its potential therapeutic applications in diseases, including Alzheimer's disease, cardiovascular diseases [9], and cancer treatment [10]. Previous studies have shown that plasma A2M levels in pregnant women with preeclampsia (PE) increased during mid- and late-pregnancy, and overexpression of A2M triggers PE-like symptoms in rats [11]. However, the precise mechanism remains unclear, and the therapeutic possibilities of targeting A2M/LRP1 in PE have not been fully explored. Although previous studies have shown that maternal inflammatory responses contribute to increased A2M levels, the exact tissue sources of A2M remain unclear. It is essential to identifying the tissue sources of A2M for developing targeted therapies.

LRP1, also known as α2-macroglobulin receptor, it mediates cytosolic action by regulates the concentrations

of extracellular ligands by transporting ligands into intracellular vesicles, additionally, it also involved in endocytosis, homeostasis, and signal transduction [12]. Up to date, the study between A2M and LRP1 are mainly focused on Alzheimer's disease, immune regulation and cancer treatment [13, 14]. Research evidence shows that when A2M and RAP are infused into the body at the same time, the binding of A2M to LRP1 in the mouse liver is significantly reduced [15], M Z Kounnas. et al.'s study revealed the role of LRP1 in Alzheimer's disease, indicating that A2M binds to β-amyloid protein (Aβ) and is cleared by LRP1, while RAP inhibits this process [16]. However, the therapeutic potential of A2M and LRP1 in preeclampsia remains unclear.

The spatiotemporal removal of vascular smooth muscle cells (VSMC) plays a crucial role in the development of defects in uterine spiral artery remodeling in PE. Apoptosis, proliferation, phenotypic switching, and abnormal migration of smooth muscle cells are pivotal processes in the replacement of uterine spiral artery smooth muscle cells. However, there remains a lack of consensus regarding the predominant phenotype involved in this process [17–19]. Emerging evidence suggests that VSMC undergo reversible changes in their biological properties, with the potential for multidirectional transformation. Specifically, VSMC transition from a contractile phenotype, which maintains vascular structure, to a synthetic phenotype characterized by undifferentiated properties. This transformation enables VSMC to migrate and secrete, ultimately leading to their gradual departure from the vessel wall during spiral artery remodeling [20]. There is no doubt that the regulation of VSMC differentiation during spiral artery remodeling has significant clinical significance. However, there is still a lack of consistent understanding of the regulatory mechanisms of VSMC disappearance disorders.

The polymerization and depolymerization of the smooth muscle cell cytoskeleton are critical mechanisms in the regulation of VSMC phenotypic switching. The polymerization of globular actin (G-actin) into filamentous actin (F-actin) activates key signaling pathways, including RhoA GTPase and MAPK. This regulatory cascade subsequently enhances the activity of nuclear transcription factors, such as serum response factor (SRF), leading to the upregulation of contractile phenotype genes, including α-SMA, while concurrently suppressing the expression of synthetic phenotype genes like osteopontin (OPN) [21, 22]. RhoA GTPase, a small GTP-binding protein belonging to the Rho family, plays a crucial role in regulating cytoskeletal dynamics, endothelial barrier function, and vascular tone. These processes are essential for maintaining normal placental development and function. Dysregulation of RhoA GTPase signaling has been implicated in various pathological conditions. Emerging evidence indicates that abnormal RhoA GTPase activity may contribute to the pathogenesis of PE by impairing trophoblast invasion, disrupting endothelial function, and inducing placental hypoxia [23, 24]. Some studies have delved deeper into the potential therapeutic applications of RhoA GTPase in PE through in vitro experimental investigations [25–27], suggesting that RhoA GTPase is a biologically validated and clinically promising therapeutic target for PE.

Thus, the present study sought to (I) elucidate the role of A2M within the progression of PE as well as to (II) explore the potential therapeutic strategies targeting A2M. A combination of bioinformatic analyses and morphological experiments, such as immunofluorescence and tunnel staining, was used to assess the relationship between A2M overexpression and SMC phenotype switching disorder during the PE progression. Additionally, proteomic analysis, LC-MS/MS analysis and Co-IP were performed to investigate the interactions involving A2M and underlying mechanisms of PE. Finally, we evaluated the therapeutic potential of blocking A2M-LRP1 by administering RAP in a preeclampsia rat model.

Materials and methods

Staging and classification of preeclampsia

Preeclampsia (PE) is a hypertensive disorder that occurs during pregnancy, characterized by new-onset hypertension and proteinuria after 20 weeks of gestation. PE is classified into two distinct subtypes based on the timing of onset: early-onset preeclampsia (EOPE) and late-onset preeclampsia (LOPE).

EOPE is defined as preeclampsia that occurs before 34 weeks of gestation, and it is typically associated with fetal growth restriction and preterm delivery, primarily linked to placental dysfunction. In contrast, LOPE occurs after 34 weeks of gestation and is generally associated with maternal factors such as metabolic abnormalities, hypertension, or obesity, exhibiting a relatively less severe clinical course and normal placental function.

Patient cohort and sample collection

Human tissue samples consisted of human blood and decidua tissue samples. This study was approved by the Ethics Committee of the First Affiliated Hospital of Jinan University (Grant number: KY-2021-092 for blood collection and KY-2021-054 for decidua collection) and were conducted in strict accordance with the Declaration of Helsinki. All study participants were duly informed, and human tissue samples were collected with their consent through signed informed consent forms. Inclusion and exclusion criteria for tissue collection were strictly adhered to as per the latest International Federation of

Obstetricians guidelines. Detailed information on the inclusion criteria of the experimental participants, as well as sample collection and storage provided in the Supplementary Material 1.

Decidual tissues from the placental junction during the third trimester, collected post-delivery, were washed three times with saline and immediately frozen at −80 °C for quantitative Western blot analysis. The samples included 30 from pre-eclampsia patients and 29 from normal subjects, with baseline data provided in Supplementary Table 2. For morphological analysis, 10 samples from pre-eclampsia patients and 10 from normal pregnant women were fixed in 4% paraformaldehyde following PBS washing, paraffin-embedded, and sectioned at 4 °C.

Decidual tissues from early pregnancy (6–8 weeks of gestation) were obtained from 15 women undergoing induced abortion. These tissues were washed and subsequently cultured for further analysis. Ten samples from each group were selected to conduct morphological experiments, following the experimental protocol outlined above.

Peripheral venous blood samples were collected during two specific gestational periods: First trimester (11 + 6 to 13 weeks of gestation): 100 samples from both pre-eclampsia and normal groups, with baseline data in Supplementary Table 3. Third trimester (4–7 days before labor onset): Samples were collected from both groups and processed as follows: they were centrifuged at 3000 g for 15 min after collection in EDTA vacuum tubes to separate plasma, which was then stored at −80 °C (baseline data in Supplementary Table 4).

Model and sample preparation of rats

SPF grade Sprague-Dawley rats (6 to 9 weeks old, weighing 180 to 200 were obtained from Vital River Laboratory Animal Technology Co., Ltd. (RRID: RGD_734476) and utilized for all animal experiments. The procedures for generating A2M overexpression rats and inducing LPS preeclampsia in pregnant rat models are detailed in the Supplementary Material 1. Animal experiments were approved by the Jinan University Animal Experimentation Ethics Committee (Grant number: IACUC-20210302-46, IACUC-20230821-04), and the experiments were conducted following the guidelines of the National Institutes of Health (NIH) Guide for the Care and Use of Laboratory Animals. Rats were categorized into respective groups and provided with nesting materials and sufficient food. At the end of the experiment, pregnant rats were anesthetized using isoflurane and euthanized by intraperitoneal injection of an overdose of pentobarbital at a dose of 150 mg/kg of body weight.

Cell culture and transfection

All details regarding cell manipulations, including cell culture conditions, consumables, and subsequent operational procedures for co-immunoprecipitation, scratch experiments, F-actin staining, Propidium Iodide (PI) staining, and flow cytometry can be found in the Supplementary Material 1. Transfection efficiency was assessed using Western blotting and is shown in Fig. S1.

Culture of decidual tissue explants in early pregnancy

The collected decidual tissues were cultured in F12 medium with 1% penicillin/streptomycin and 10% fetal bovine serum (FBS). Decidual secretions were extracted following established methods [28, 29]. Briefly, finely minced and trimmed decidua was evenly distributed in the upper part of a 12-well plate transwell chamber with a mixture of 10% FBS, F12, 20ng/ml progesterone, and 300pg/mL 17β-estradiol in a 1:1 matrix gel and serum-free F12 medium. The lower chamber contained DMEM. Multi-tissue coculture was maintained for one week before proceeding with further experiments.

Vascular explant model

Intact chorionic plate arteries were isolated from term placentas and cultured in a cell incubator. After 24 h of serum deprivation, the arteries were exposed to various conditioned media. Subsequently, after 120 h, the arteries were harvested and embedded in paraffin for morphological analysis [28, 29].

Histological analysis

Histological analysis included immunohistochemistry, immunofluorescence and TUNEL staining. Specific statistical methods and operational details are described in Supplementary Material 1.

Quantitative analysis

Western blotting (WB), Polymerase chain reaction (PCR), and ELISA were employed for quantitative analysis of protein levels of specific genes, mRNA quantification, and measuring the concentration of A2M in plasma, respectively. For detailed operating procedures and information on consumables, please refer to the Supplementary Material 1.

Bioinformatics analysis

Various bioinformatics analysis techniques were utilized in this study, including LC-MS/MS analysis, single-cell data set analysis (Dataset number: GSE214607) [30], Protein-Protein Docking, Protein-protein Interaction Network (PPI) construction, proteomic sequencing of rat decidua tissue. The performance of the diagnostic model was assessed using Kaplan-Meier (K-M) Analysis

and time-dependent ROC curves. All analyses were conducted using R software (version 4.3.3) and specific details are provided in the Supplementary Material 1.

Statistical analysis

Statistical analyses were performed using SPSS 26 software and are expressed as mean ± SEM. Data were first normalized, and tested for homogeneity of variance and normality. Wilcoxon rank-sum test was utilized for non-normally distributed data with non-homogeneous variance, while the t-test was applied for normally distributed data with homogeneous variance. Significance levels were indicated as * for $p < 0.05$, ** for $p < 0.01$, and *** for $p < 0.001$.

Results

Phenotypic switching-driven emigration predominates vascular smooth muscle cell loss in spiral artery remodeling

Spiral arterial remodeling (SPA-REM) is a common phenomenon in patients with PE and is characterized by a lower proportion of appropriately remodeled spiral arteries. This dysregulation is associated with impaired SMC loss within the arterial wall. In this study, we systematically reviewed articles published over the past five years regarding the mechanisms underlying smooth muscle cell regression disorders in the wall of the uterine spiral artery (refer to Fig. S2-S3 for a detailed analysis process). Our findings indicate that phenotype switching and apoptosis are the most recognized mechanisms of smooth muscle cell regression in this context, with a notable increase in the number of studies focusing on phenotype switching each year. By utilizing immunofluorescence and Tunnel staining, SMC apoptosis and migration induced by phenotypic conversion during spiral artery remodeling were further evaluated (Fig. 1B). According to the quantitative analysis, during the remodeling process of SPA vascular wall, the proportion of SMC undergoing phenotypic switching was higher than the proportion of SMC undergoing apoptosis (Fig. 1C).

In order to investigate the impact of SMC phenotype switching on spiral artery remodeling, a single-cell RNA-seq data analysis was performed on decidual tissue samples from early pregnancy (Fig. 1D). Then the analysis focused on cells identified as smooth muscle cells for cluster analysis was performed, the identification of single-cell transcriptome data clusters is detailed in Fig. S4 A-G. Pseudo-chronological clustering analysis indicated that SMC phenotype switching occurs alongside the primary direction of SMC differentiation, gradually replacing contractile phenotype smooth muscle cells over time (Fig. 1E). Together, these results revealed that SMC phenotype switching is the main fate of SMC during uterine SPA-REM (Fig. 1F).

A2M is upregulated in smooth muscle cells of uterine spiral artery walls in patients with PE and its association with smooth muscle phenotype switching disorder

Increased A2M expression in decidual tissue and uterine spiral artery smooth muscles in patients with PE is positively correlated with the severity of spiral artery remodeling (Fig. 2A-D). Temporal analysis indicates a strong correlation between A2M expression and markers of smooth muscle contractile phenotype (Fig. 2E). Immunofluorescence staining of A2M and α-SMA confirms increased expression in vascular smooth muscle cells without phenotypic switching, additionally, fluorescence intensity analysis is consistent across different centrifugal distances (Fig. 2F-H), a significant positive correlation between fluorescence intensity of A2M and α-SMA was observed ($R = 0.51$, $P < 0.05$) (Fig. 2I).

A2M overexpression suppresses uterine spiral artery remodeling by hindering phenotypic switching of vascular smooth muscle cells

To study the role of A2M in SPA-REM, A2M overexpression rats were studied, resulted in a phenotype similar to that of PE, which is characterized by impaired SPA-REM in both early and late pregnancy rats' mesometrial triangle and superficial muscle layers (Fig. 3A-F). This indicates that A2M overexpression may play a role in inhibiting SPA-REM and contributing to the pathogenesis of PE.

Based on the observations in rat model decidual tissue, late-pregnancy rats with A2M overexpression exhibited more severe phenotypic switching disorders in spiral artery smooth muscle cells (Fig. 3G). Specifically, there was a higher α-SMA fluorescence intensity in the decidua and superficial muscle layer (Fig. 3H), as well as a greater proportion of impaired phenotype switching in the arterial wall helices. These cells displayed elongated spindle-shaped morphologies and a decrease in rounded or displaced cells when A2M was overexpressed (Fig. 3I, J).

Proteomic sequencing analysis was performed on rat mesometrial triangle and superficial uterine myometrium tissues. Gene Ontology (GO) analysis (Fig. 3K) identified ten significantly altered biological processes in the decidual tissues of rats with A2M overexpression, with a significant mechanism linked to smooth muscle cell phenotypic switching. Kyoto Encyclopedia of Genes and Genomes (KEGG) analysis indicated that A2M overexpression may impact the cellular cytoskeleton through the 'Regulation of cytoskeleton' pathway (Fig. 3L). MCC analysis highlighted RhoA, Rac1, and CDC42 as the top

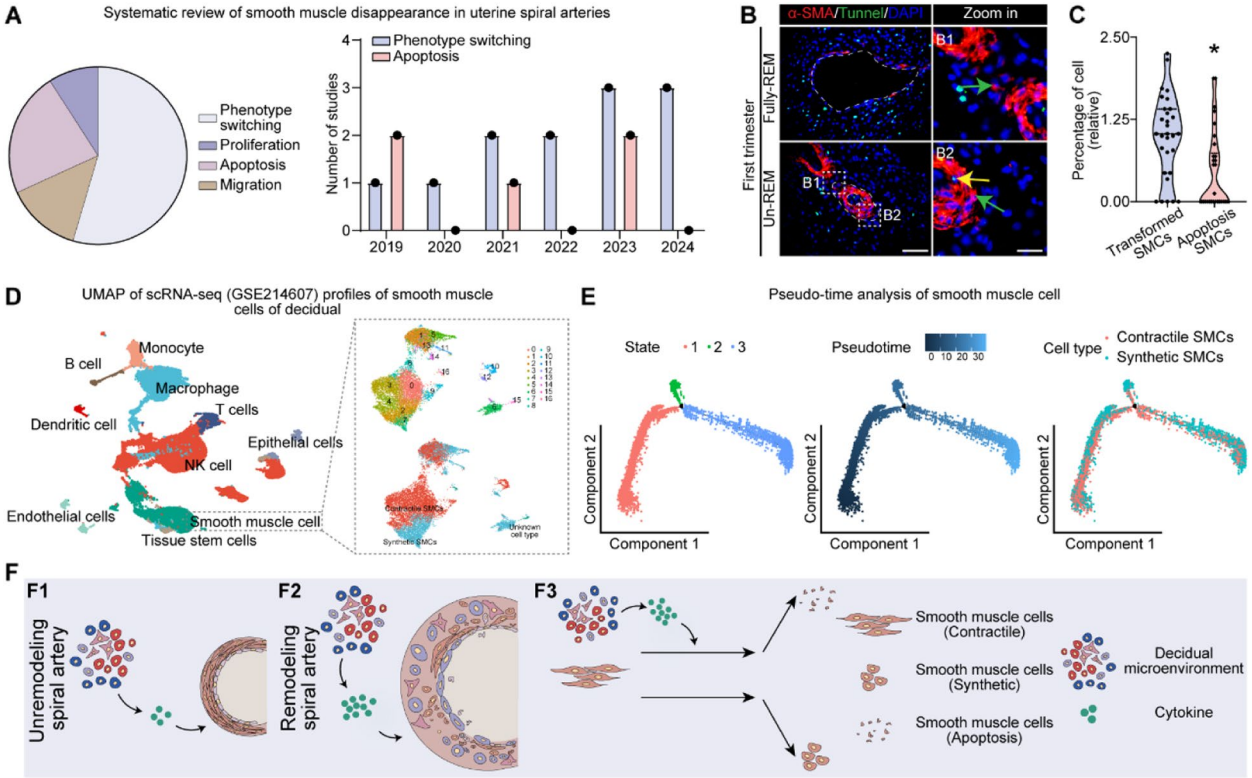

Fig. 1 Smooth muscle cell phenotype switching: key mechanism in uterine spiral artery remodeling. **A** Systematic reviews indicate that SMC apoptosis and phenotypic transformation have garnered significant attention in the context of uterine spiral artery remodeling. Furthermore, the number of studies focusing on smooth muscle cell phenotypic transformation has shown a consistent annual increase. **B**, **C** In first trimester, the proportion of SPAs-SMC undergoing phenotype switching is higher than that of apoptotic SPAs-SMC (Each group included 15 participants, and two sections from different parts were randomly selected for each participant. In Fig. 1B1 and B2, green arrows point to SMC that have undergone phenotypic switching, yellow arrows point to SMC that have undergone apoptosis). **D** UMAP visualization of the human decidual cell atlas single-cell transcriptomics data colored by cell type, SMC were identified and categorized into contractile and synthetic phenotypes based on the expression of distinct marker genes. **E** Pseudo-time analysis for the transition of SMC from a contractile phenotype to a synthetic phenotype in the early pregnancy (The timeline progresses from left to right, with state 1 in the leftmost chart representing the earliest stage along the developmental axis, while state 3 represents a later stage in the progression). **F** Dynamic changes of SPAs-SMC during SPA-REM process. The statistical methods used in the figures are all adjusted *p*-values obtained by the nonparametric Wilcoxon rank-sum test and Bonferroni correction, data represent the mean ± SD, ns $P > 0.05$, * $P < 0.05$, ** $P < 0.01$, *** $P < 0.001$. SPAs (Spiral artery), SPA-REM (Spiral artery remodeling), SMC (Smooth muscle cells), UMAP (Uniform Manifold Approximation and Projection), α-SMA (α-smooth muscle actin), CK7 (Cytokeratin 7)

three hub genes within the enriched pathways (Fig. 3M, N), with gene expression shown in Fig. 3O.

A2M overexpression suppresses smooth muscle cell phenotypic switching by upregulating the RhoA GTPase pathway

Upregulating A2M expression inhibited rat aortic smooth muscle cells (RASMC) phenotypic switching, resulting in reduced cell migration ability, increased contractile phenotype markers, and decreased synthetic phenotype markers (Fig. 4A-F). Conversely, A2M knockdown led to a higher degree of synthetic phenotype transition in RASMC.

F-actin and G-actin staining demonstrated that G-actin aggregation induced RASMC to contract and adopt a contractile phenotype. A2M overexpression promoted F-actin formation but inhibited G-actin depolymerization, resulting in increased F-actin fluorescence intensity and decreased G-actin fluorescence intensity. Conversely, downregulating A2M significantly increased G-actin fluorescence intensity while decreased F-actin fluorescence intensity. This reveals the role of A2M in maintaining the contractile phenotype by enhancing cytoskeletal aggregation (Fig. 4G-I).

In addition, we also explored the effect of A2M on RASMC apoptosis. In the rat decidual tissue, we observed that A2M overexpression reduced Caspase 3 expression surrounding spiral artery walls (Fig. S5A-B). Western blotting on rat decidual tissue indicated that A2M downregulated Caspase 3 while upregulated Bcl-2

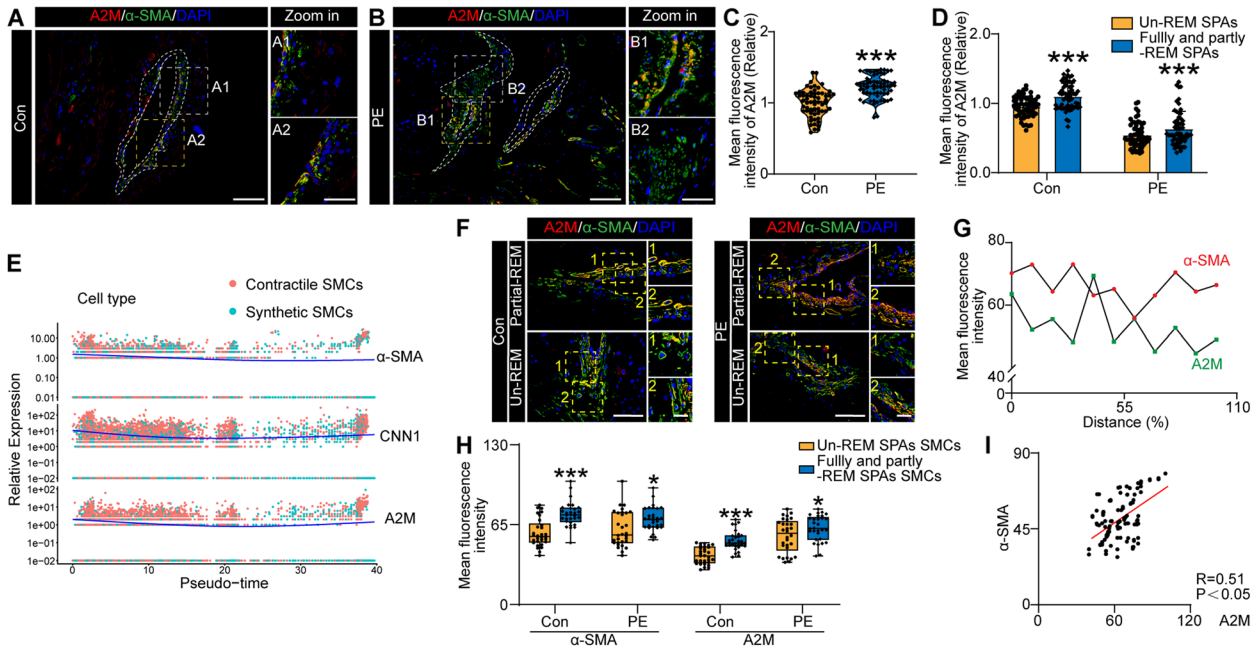

Fig. 2 A2M is upregulated in smooth muscle cells of uterine spiral artery walls in patients with PE and Its association with smooth muscle phenotype switching disorder. **A** Representative images of A2M (red), α-SMA (green) and DAPI (blue) staining of uterine SPAs for normal pregnancy and (**B**) PE (The scale bar measures 175 μm, while the scale bar in the enlarged image on the right measures 75 μm. Each group consisted of 30 participants in the third trimester. For each participant, two morphologically intact decidual tissue sections from different regions were selected, and two random fields of view were chosen for quantitative analysis from each section). **C** Higher fluorescence intensity of A2M in the SMC of the decidual SPAs wall in pregnant women with PE. **D** Higher A2M fluorescence intensity in the smooth muscle of the SPAs wall with less remodeling. **E** Pseudo-time analysis showing consistent expression trends of A2M, α-SMA, and CNN1 in SMC. **F** Representative images of α-SMA (green), A2M (red) and DAPI (blue) staining of SMC at different levels of phenotype switching (The scale bar measures 90 μm, while the scale bar in the enlarged image below measures 40 μm. Each group consisted of 15 participants in the first trimester, and two sections from distinct regions were randomly selected for each participant. In the diagram, "1" indicates SMC that have undergone phenotype switching, while "2" denotes SMC that have retained their original phenotype without undergoing phenotype switching). **G** Unchanged of α-SMA and A2M fluorescence intensities with the cell centrifugal distance. **H** Higher fluorescence intensity of A2M in the SMC of the uterine SPAs with less phenotype switching (no displacement, spindle shape); **I** Pearson's r correlations for fluorescence intensity of A2M and α-SMA in human decidual uterine SPAs. Data represent the mean ± SD, ns $P > 0.05$, * $P < 0.05$, ** $P < 0.01$, *** $P < 0.001$. PE (PE), A2M (α2-macroglobulin), α-SMA (α-smooth muscle actin), CNN1 (Calponin 1), SMC (Smooth muscle cells), SPAs (Spiral artery)

(See figure on next page.)

Fig. 3 A2M overexpression suppresses rat spiral artery remodeling and smooth muscle cell phenotype switching. **A**-**C** Representative images of immunostained for α-SMA of placenta-decidua tissues of Ad-ctrl and Ad-A2M rats in early pregnancy. **D**-**F** Representative images of immunohistochemistry of placenta-decidua tissues of Ad-ctrl and Ad-A2M rats in early pregnancy (**A**, **B**, **D**, **E**) The scale bar is 300 μm, with the scale bar after enlargement being 50 μm, n=6. **C**, **F** Each group contained 6 rats, with 5 placenta-myometrium complexes randomly selected from each rat for morphological observation. Five fields of view were analyzed per complex, and results were presented as percentage stacked graphs). **G** Immunofluorescence staining of rat decidual and myometrium SPAs for α-SMA (red), CK7 (green) and DAPI (blue). **H**-**J** The fluorescence intensity of α-SMA in the decidua and superficial myometrium increased in the Ad-A2M group. **I** The decrease of the number of round smooth muscle cells in the decidua and superficial myometrium Ad-A2M group; **J** The increase of the number of spindle smooth muscle cells in the decidua and superficial myometrium in Ad-A2M group. Each group contained 6 rats, with 5 placenta-myometrium complexes randomly selected from each rat for morphological observation. Five fields of view were analyzed per complex. Each point in the statistical graph represents the average observation of a placenta-myometrium complex (The scale bar is 90 μm). **K** GO analysis of proteomic sequencing indicated that A2M overexpression may influence the phenotypic switching of smooth muscle cells by regulating processes such as cell morphology and actin filament organization. **L** Further KEGG analysis suggesting that A2M may affect actin filament organization through the actin cytoskeleton pathway. **M** Analysis of protein-protein interaction networks, **N** the MCC algorithm demonstrates the top 20 hub genes, with RhoA, CDC42, and Rac1 ranking highest. **O** Heatmap shows expression levels of genes in the networks. Significance levels indicated as *$P < 0.05$, ** $P < 0.01$, *** $P < 0.001$. Error bars represent the mean ± SD. A2M (α2-macroglobulin), α-SMA (α-smooth muscle actin), CK7 (Cytokeratin 7), GD (Gestational Day), MCC (Maximum Clique Centrality), GO (Gene Ontology), KEGG (Kyoto Encyclopedia of Genes and Genomes), RhoA (Ras Homolog Family Member A), mDia (Diaphanous-related formin 1), CDC42 (Cell Division Cycle 42)

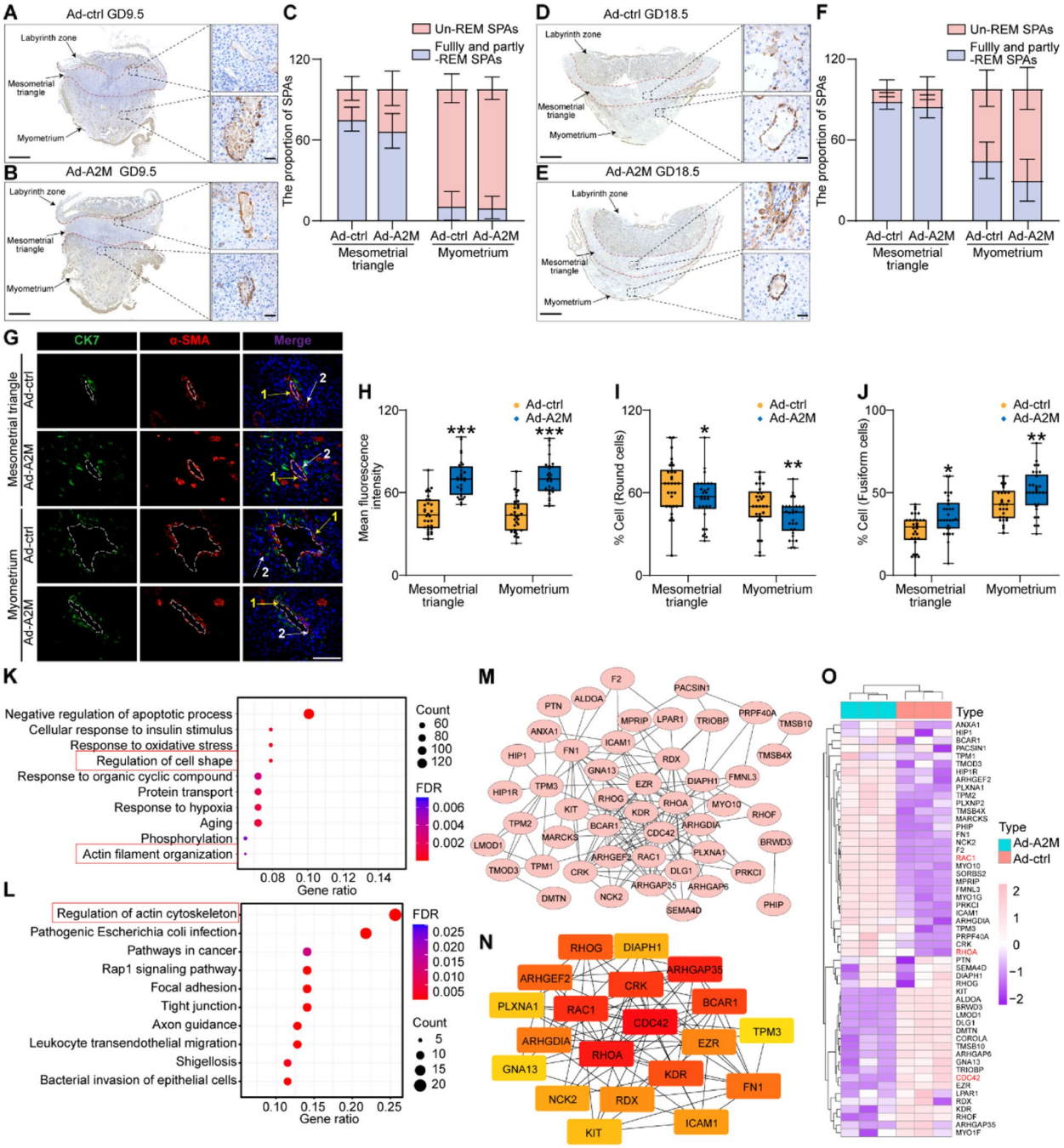

Fig. 3 (See legend on previous page.)

expression (Fig. S5C-D). A2M overexpression inhibited RASMC apoptosis, while A2M knockdown increased apoptosis. PI assay demonstrated lower PI-positive cells with A2M overexpression and higher with A2M knockdown (Fig. S5E and F). Similar protein-level results can be found (Fig. S5G-H), with A2M overexpression increasing Bcl-2 expression and decreasing CASP3 expression. Flow cytometry showed more cells in the Q2 region with A2M overexpression and fewer with shA2M (Fig. S5I). On the other hand, these results were supported by the PCR (Fig. S5J).

A2M interacts directly with RhoA GTPase and promotes RhoA GTPase activation

According to current knowledge, Rac1 and CDC42 are primarily involved in pseudopodia formation at the cell

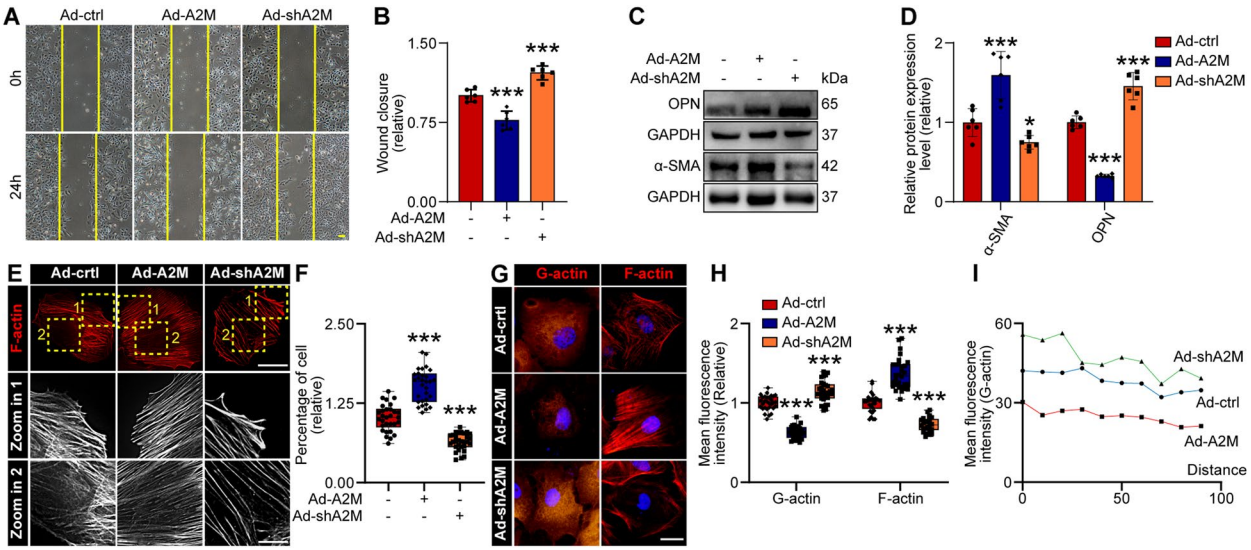

Fig. 4 A2M is involved in the regulation of smooth muscle cell phenotype switching by promotes cytoskeleton polymerization. **A** Representative images of scratch assays to evaluate the effects of A2M on RASMC migration (Scale bar=100μm, repeat the experiment *n*=6); **B** A2M inhibited the migration ability of RASMC, and knockdown of A2M enhanced the migration ability of RASMC. **C**, **D** Western blot analysis demonstrating that A2M promoted the expression of contractile phenotype markers (α-SMA) and reduced synthetic marker expression (OPN). **E** Representative F-actin staining illustrated the effects of A2M on RASMC stress fibers (Scale bar=25μm). **F** Morphological observations indicating an increase in spindle cells and F-actin intensity with A2M overexpression. **G-I** Assessment of A2M effect on G- and F-actin fluorescence in RASMC (Scale bar=25μm, repeat the experiment *n*=6). A2M (α2-macroglobulin), RASMC (Rat thoracic aortic smooth muscle cell), OPN (Osteopontin), α-SMA (α-smooth muscle actin), RhoA (Ras Homolog Family Member A), mDia (Diaphanous-related formin 1)

periphery, while RhoA mainly contributes to stress fiber formation in the cell center (Fig. 5A). F-actin fluorescence results suggested that A2M overexpression did not significantly increase pseudopodia formation (Fig. 5B and C), indicating that A2M may primarily regulate RhoA GTPase activity.

Western blotting on human decidual tissue showed that A2M, RhoA, and mDia were upregulated and positively correlated in patients with PE (Fig. 5D-G). A2M overexpression increased RhoA and mDia protein levels, while A2M knockdown decreased their expression in smooth muscle cells (Fig. 5H, I). Further cell fluorescence experimental results suggest that A2M and RhoA are concentrated in the cytoplasm of RASMC (Fig. 5J).

To gain insight into the molecular mechanism between A2M and RhoA, protein-protein docking was performed (All LC-MS/MS analysis results are provided in Supplementary Material 2), and results suggest that A2M can stably bind to RhoA (Fig. 5K). To identify potential substrate proteins regulated by A2M, we used A2M immunoprecipitation coupled with mass spectrometry. Of the potential A2M binding proteins, RhoA piqued our interest as it has the highest sequest HT score (Fig. 5L). Further, the immunoprecipitation experiments result demonstrated binding between A2M and RhoA in RASMC, and direct binding could be observed between RhoA and A2M (Fig. 5M, N).

The decidual tissue secretions fail to rescue A2M overexpression-induced inhibition of smooth muscle cell phenotypic switching

To investigate whether the effect of A2M on RASMC can be changed by the physiological environment of decidua, a Placenta Decidual Co-culture (PDC) model was established (Fig. 6A). Cytological experiments showed that decidual tissue secretions promoted smooth muscle cell migration and synthetic phenotypic marker expression, but did not reverse the effects of A2M on smooth muscle cells, resulting in inhibited migration and increased expression of smooth muscle contraction phenotype markers (Fig. 6B-E). Additionally, in a chorionic villus artery transplantation model, the PDC serum increased the proportion of synthetic phenotype smooth muscle cells while decreased spindle-shaped smooth muscle cells. However, this failed to rescue A2M overexpression-induced phenotypic switching (Fig. 6F, I).

In addition to focusing on the phenotype switching of RASMC, we also paid attention to the effect of apoptosis of RASMC. PDC serum could not counteract the inhibitory effect of A2M on apoptosis. Despite a significant increase in the proportion of PI-positive cells, decidual tissue failed to rescue the inhibitory effect of A2M on smooth muscle cell apoptosis in the PI assay (Fig. 6J-K). Western blotting confirmed that A2M promoted CASP 3 expression while inhibiting

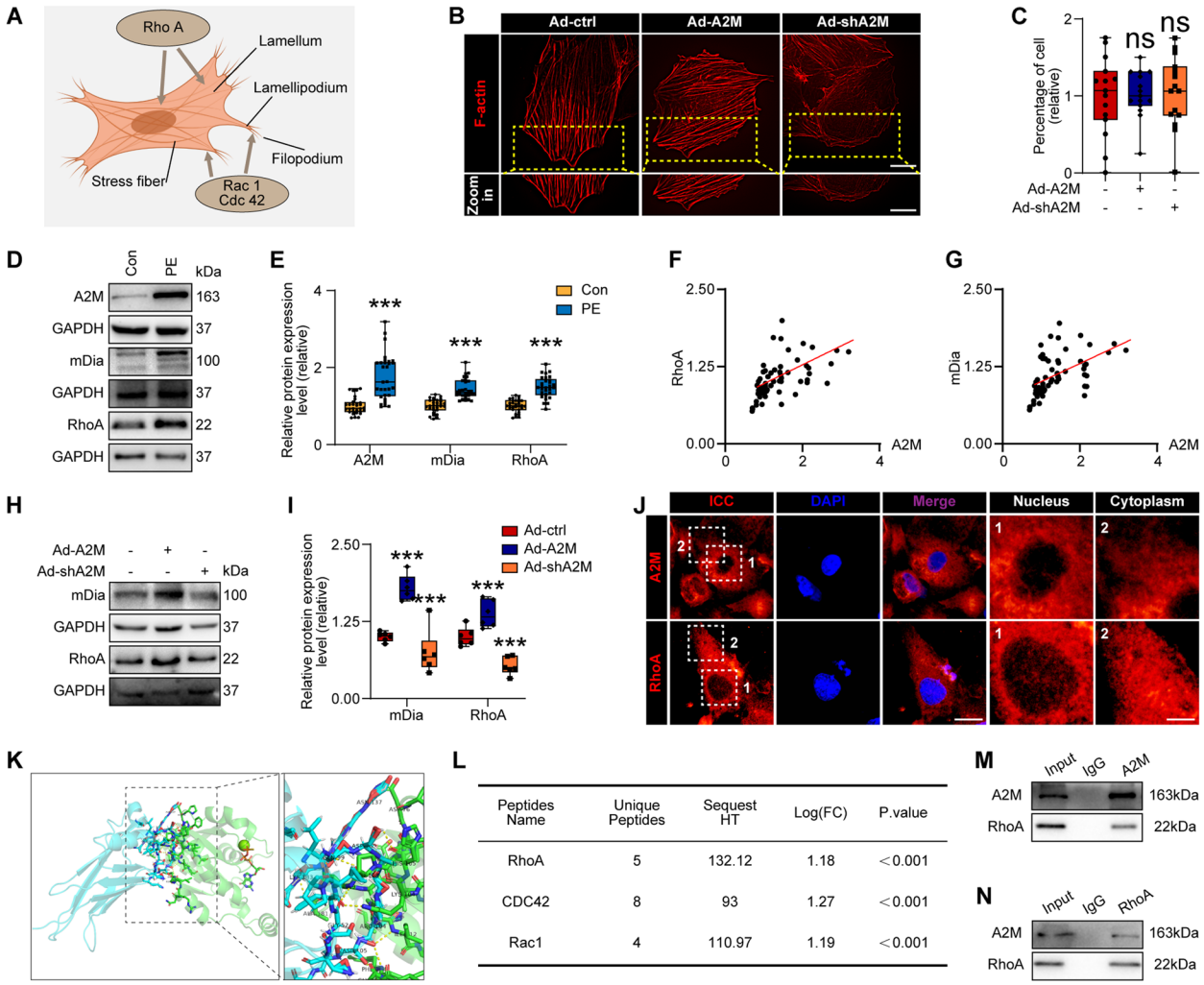

Peptides Name	Unique Peptides	Sequest HT	Log(FC)	P.value
RhoA	5	132.12	1.18	<0.001
CDC42	8	93	1.27	<0.001
Rac1	4	110.97	1.19	<0.001

Fig. 5 A2M interacts directly with RhoA GTPase and promotes RhoA GTPase activation. **A** RhoA GTPase primarily regulates the formation of stress fibers and the lamellar cytoskeleton in SMC, whereas Rac1 and CDC42 are predominantly involved in promoting the formation of lamellipodia and filopodia cytoskeletal structures. **B** Representative immunofluorescence images of F-actin (red, the scale bars in the bove and below images are both 25μm, *n*=6). **C** Ad-A2M or Ad-shA2M did not affect the formation of pseudopodia in the edge of RASMC. **D**-**E** Representative immunoblots of A2M, RhoA, and mDia from human decidual and the quantified ratio of A2M/GAPDH, RhoA/GAPDH and mDia/GAPDH (*n*=30 for each group). **H**-**I** Representative immunoblots of RhoA, and mDia from RASMC, the quantified ratio of RhoA/GAPDH and mDia/GAPDH. **J** Representative images of A2M (red, the upper line), RhoA (red, the downlink), and DAPI (blue), (the scale bars are 25μm, with the scale bar after enlargement being 50μm, repeat the experiment *n*=6). **K** Molecular docking of A2M and RhoA. **L** Selected peptide hits of Rho GTPase family proteins associated with A2M were identified through mass spectrometry analysis. **M**-**N** Immunoprecipitation results showing that A2M and RhoA can bind to each other directly (repeat the experiment *n*=6). Error bars, mean ± SD, with significance levels indicated as * $P < 0.05$, ** $P < 0.01$, *** $P < 0.001$. A2M (α2-macroglobulin), RhoA (Ras Homolog Family Member A), mDia (Diaphanous-related formin 1), CDC42 (Cell Division Cycle 42), SMC (Smooth muscle cells), RASMC (Rat thoracic aortic smooth muscle cell)

Bcl-2 expression at the protein level (Fig. 6L, M). Flow cytometry results showed an increase in cells in the Q2 zone with decidual tissue secretions, but this did not reverse the decrease observed in the A2M overexpression group. Overall, there was limited rescuing effect of decidual tissue secretions on endogenous A2M overexpression (Fig. 6N). Nevertheless, our data indicates that PDC serum do not exist an influence on smooth muscle's A2M expression (Fig. 6O). In conclusion, these results indicate that, in a physiological environment, decidual tissue secretions cannot alter the inhibitory effects of A2M on the phenotypic transition and apoptosis of RASMC.

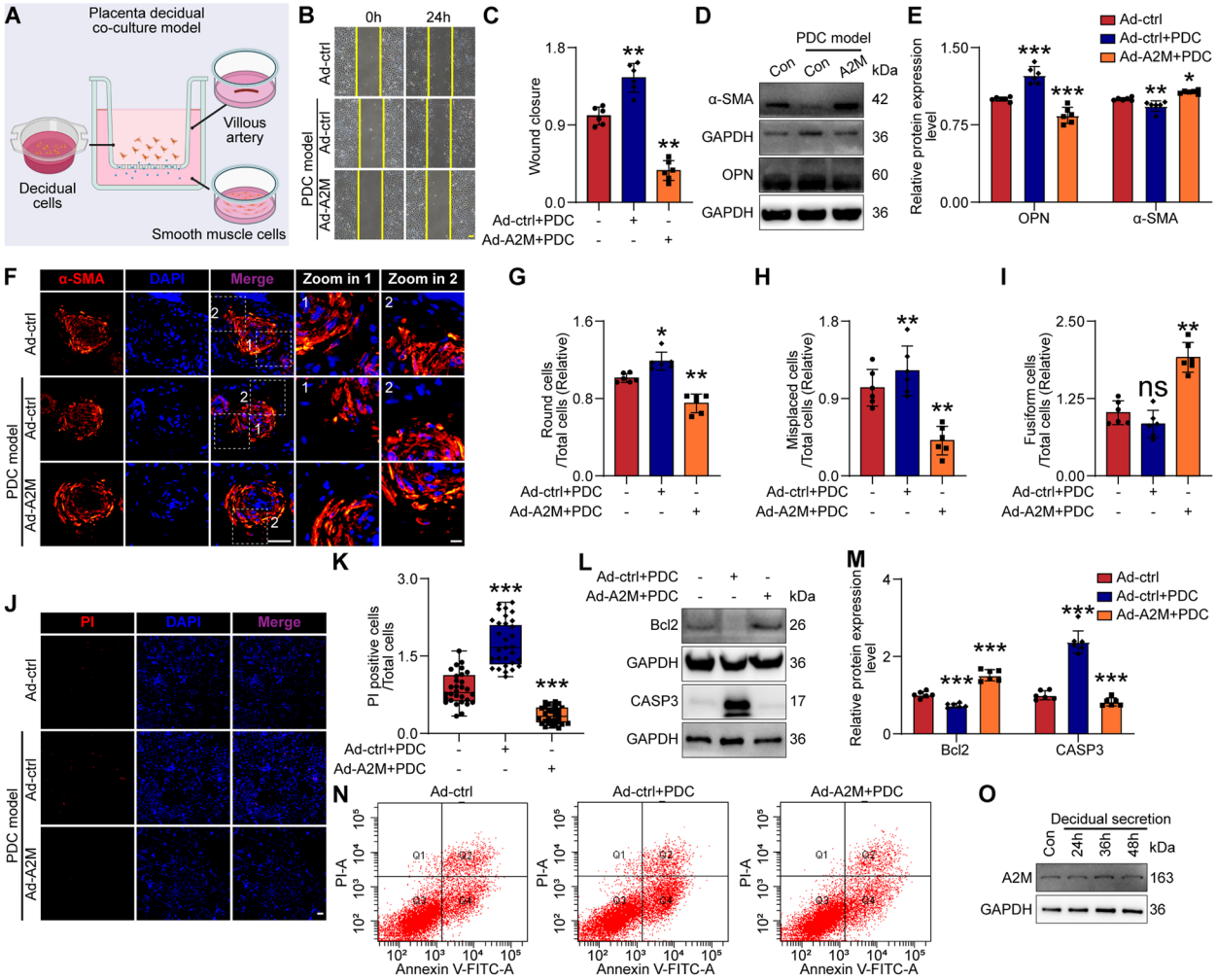

Fig. 6 Placenta decidual co-culture medium fail to rescue A2M's inhibition of smooth muscle cell phenotypic switching and apoptosis. **A** Schematic illustration of experiments. **B**, **C** Scratch assay evaluating RASMC migration (Scale bar=100μm, repeat the experiment *n*=6). **D**, **E** Representative immunoblots of α-SMA, OPN from human decidual and the quantified ratio of α-SMA/GAPDH, OPN/GAPDH (Repeat the experiment *n*=6). **F** Representative immunofluorescence staining of α-SMA (red), DAPI (blue) of chorionic villus artery transplantation model. **G**-**I** Quantitative analysis of the proportion of round SMC, displaced SMC, and fusiform SMC in the chorionic villus artery transplantation model. **J**, **K** PI staining assessing RASMC apoptosis rate (Scale bar=100μm, repeat the experiment*n*=6). **L**, **M** Representative immunoblot of RASMC, PDC medium up-regulated CASP3 and down-regulated Bcl-2 expression. **N** Representative images of Flow cytometry showing that PDC medium promoted RASMC apoptosis, whereas A2M+PDC medium reducing it (Repeat the experiment *n*=6). **O** Representative immunoblot of A2M in RASMC (Repeat the experiment *n*=6). Error bars, mean ± SD, with significance levels as * $P < 0.05$, ** $P < 0.01$, *** $P < 0.001$. PDC model (Placenta decidual co-culture model), A2M (α2-macroglobulin), RASMC (rat thoracic aortic smooth muscle cell), OPN (Osteopontin), α-SMA (α-smooth muscle actin), PI (Propidium Iodide Apoptosis Assay), CASP3 (Caspase-3), Bcl-2 (Bcl-2 apoptosis regulator)

Blocking A2M/LRP1 interaction effectively alleviate smooth muscle cell phenotype switching disorder

Single-cell transcriptome analysis revealed co-localization of A2M and its receptor LRP-1 in macrophages and smooth muscle cells within decidual tissue (Fig. 7A-D). Current understanding suggests that the RAP primarily inhibits the A2M/LRP-1 interaction by competitively binding to LRP-1 (Fig. 7E). Further immunofluorescence experiments confirmed A2M and LRP-1 expression in smooth muscle cells of the uterine spiral artery wall. Comparison of LRP-1 fluorescence intensity in decidual tissue of preeclamptic and normal pregnant women showed no significant difference (Fig. 7F-I). Morphological observations of villous artery transplantation model demonstrated that RAP protein more effectively inhibited the contractile phenotype of SMC in the vessel wall compared to A2M gene knockdown (Fig. 7J, K). At the same time, the experimental results of qPCR (Fig. S6A), Western blotting (Fig.

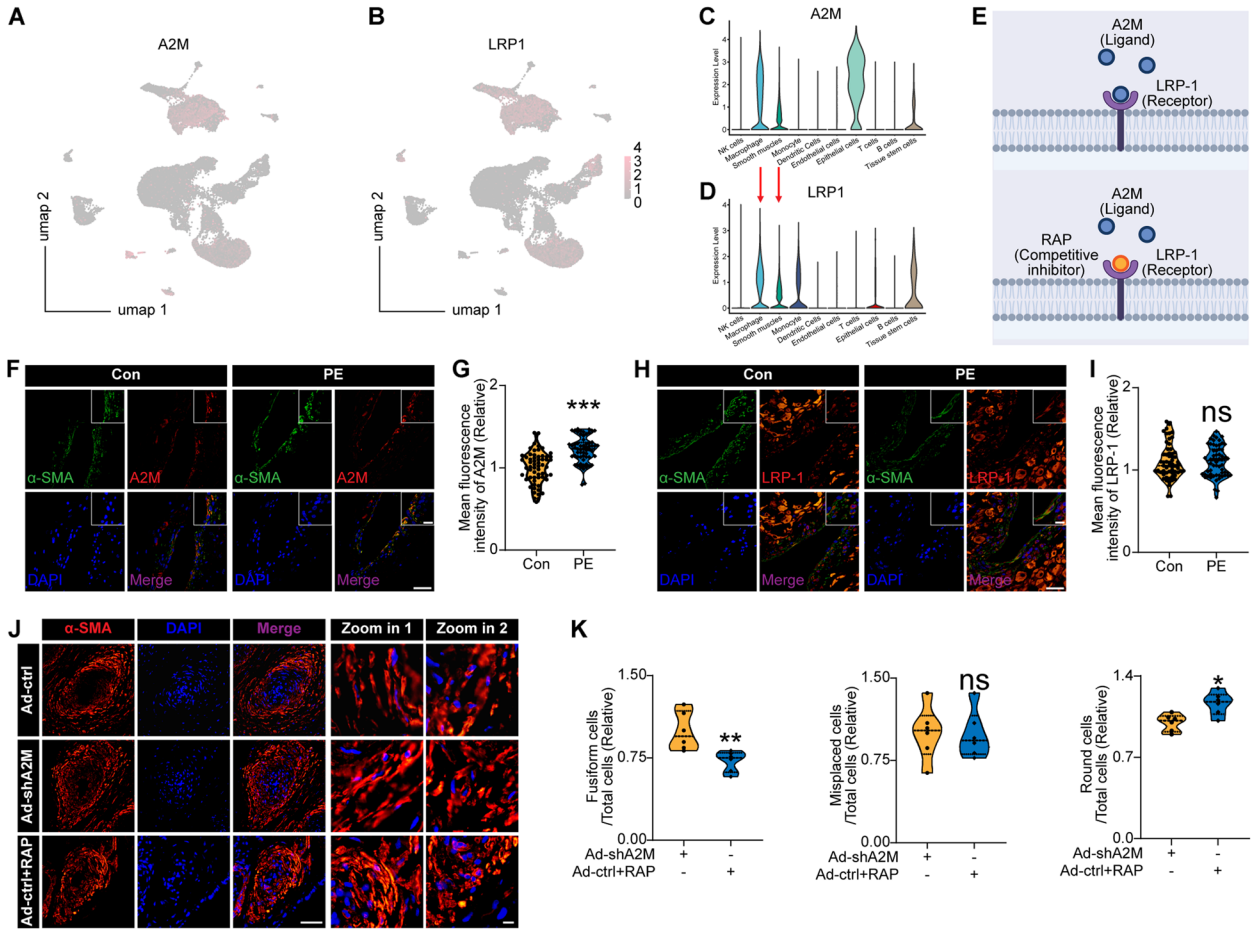

Fig. 7 Blocking A2M/LRP1 interaction effectively alleviate smooth muscle cell phenotype switching disorder. **A**, **B** Single-cell transcriptome analysis predicting the localization of A2M and its receptor LRP-1 in decidua. Violin plots depicted the gene expression profiles of A2M (**C**) and LRP-1 (**D**). **E** A schematic diagram for the competitive inhibition of A2M-LRP-1 by RAP. **F**, **G** Representative immunofluorescence staining of α-SMA (green), DAPI (blue) and A2M (red), with higher fluorescence intensity observed in PE. **H**, **I** Representative immunofluorescence staining of α-SMA (green), DAPI (blue) and LRP-1 (red) (F-I: Scale bar=100μm, the scale bar in the enlarged image is 35μm, Decidual tissues from 30 participants were selected, including 15 patients with PE and 15 normal pregnant women. Two complete tissue sections were randomly chosen from each participant, and two fields of view were randomly selected from each section for observation). **J**, **K** Representative images of villous vascular explants (Scale bar=100μm, the scale bar in the enlarged image is 90μm) showing that RAP promoted the presence of round smooth muscle cells and reduced spindle cells in the vascular wall. Six explant models were selected for each group, with three fields of view randomly selected from each model for statistical analysis, each point in the statistical graphs represented the average observation value of one explant model. Error bars, mean ± SD, with significance levels of * $P < 0.05$, ** $P < 0.01$, *** $P < 0.001$. LRP-1 (Low Density Lipoprotein Receptor-Related Protein 1), A2M (α2-macroglobulin), RAP (Receptor-associated protein), α-SMA (α-smooth muscle actin)

S6B-C) and flow cytometry (Fig. S6D) showed that RAP promoted the apoptosis of RASMC.

Receptor-associated proteins exacerbated SMC phenotype switching with reduce RhoA GTPase pathway activity

Since knockdown A2M can reduce RhoA GTPase pathway activation, we sought to investigate the effect of RAP on it. Firstly, the results at the cytological level by PCR and Western blot experiments, revealing the inhibition of RAP on contractile phenotype markers and increased expression of the synthetic phenotype marker osteopontin (Fig. 8A-C). Then, the migration ability of RASMC in scratch experiments provide evidence to support the above conclusion (Fig. 8D, E).

Cell fluorescence experiment results indicate that RAP can significantly reduce the fluorescence intensity of F-actin (Fig. 8F, G). In addition, we observed that the proportion of RASMC with round shape and fewer stress fibers increased in the RAP intervention group (Fig. 8H). In addition, RAP intervention did not increase the proportion of RASMC with pseudopodia (Fig. 8I). Furthermore, the experimental results suggest that RAP

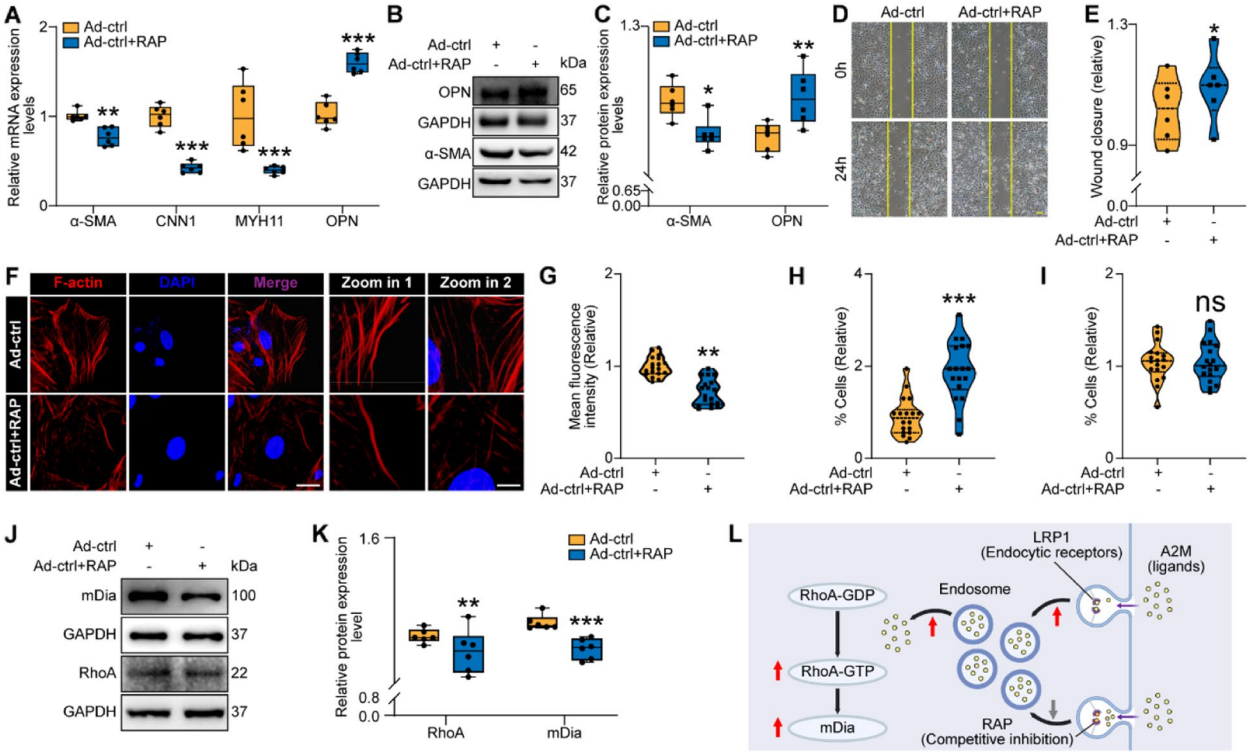

Fig. 8 Receptor-associated proteins exacerbated SMC phenotype switching with reduce RhoA GTPase pathway activity. **A** The levels of α-SMA, CNN1, MYH11 and OPN were determined by qPCR.**B**-**C** Representative immunoblot of α-SMA and OPN on RASMC. **D**-**E** Scratch assay evaluating RASMC migration (Scale bar=100μm, repeat the experiment *n*=6). **F** Representative images of F-actin (red) and DAPI (blue) on RASMC (the scale bars are 25μm, with the scale bar after enlargement being 50μm, repeat the experiment *n*=6). **G** Quantification of mean optical density values of F-actin. **H** Proportion of round RASMC. **I** The proportion of RASMC with lamellipodia.**J**, **K** Representative immunoblot of RhoA and mDia on RASMC. **L** Schematic representation of the mechanism by which RAP blocks the binding of A2M to LRP-1 and modulates the activity of the RhoA GTPase pathway. A2M (α2-macroglobulin), α-SMA (α-smooth muscle actin), CNN1 (Calponin 1), MYH11 (Myosin Heavy Chain 11), OPN (Osteopontin), RhoA (Ras Homolog Family Member A), mDia (Diaphanous-related formin 1), CDC42 (Cell Division Cycle 42), RASMC (Rat thoracic aortic smooth muscle cell), RAP (Receptor-associated protein)

intervention significantly reduces the expression of mDia and RhoA at the protein level in RASMC (Fig. 8J, K). The above experimental results indicate that blocking A2M-LRP binding can significantly reduce the activity of the RhoA-GTPase pathway (Fig. 8L).

Receptor-associated proteins can rescue related disease phenotypes in pre-eclampsia rats

To study the therapeutic potential of RAP for preeclampsia, we constructed LPS preeclampsia rat model, then injection of RAP via tail vein (Fig. 9A). According to the protein-protein interaction analysis, it is clear that RAP effectively binds to both A2M and LRP-1 (Fig. 9B). In the PE rat model induced by LPS, maternal blood pressure levels were reduced after tail vein injection of RAP, validating the initial hypothesis (Fig. 9C, D). Ultrasound evaluation of rat uterine artery pulsatility index and resistance index showed significant decreases with RAP treatment in LPS-induced preeclampsia (Fig. 9E-G). In statistical analysis, fetal and placental size/mass in the RAP-administered group is smaller compared to controls, along with reductions in fetal crown-rump length and placental diameter. Moreover, fewer offspring per litter were observed in the LPS group compared to controls. Although RAP administration increased placental size and weight of LPS-treated rats towards control levels, full restoration was not achieved (Fig. 9H, I). This suggests that RAP partially rescues the LPS-induced PE phenotype. Furthermore, RAP increased the number and proportion of remodeled spiral arteries in the superficial uterine myometrium, although slightly lower than controls (Fig. 9J-L).

As shown in morphological analysis images, RAP administration enhanced the inhibition of round cell proportion caused by LPS, although not fully restored to control levels. The proportion of displaced and spindle smooth muscle cells in spiral arteries of the superficial uterine myometrium in the RAP+LPS group is similar to that of controls (Fig. 9M, N). In conclusion, RAP administration partially mitigates the preeclampsia

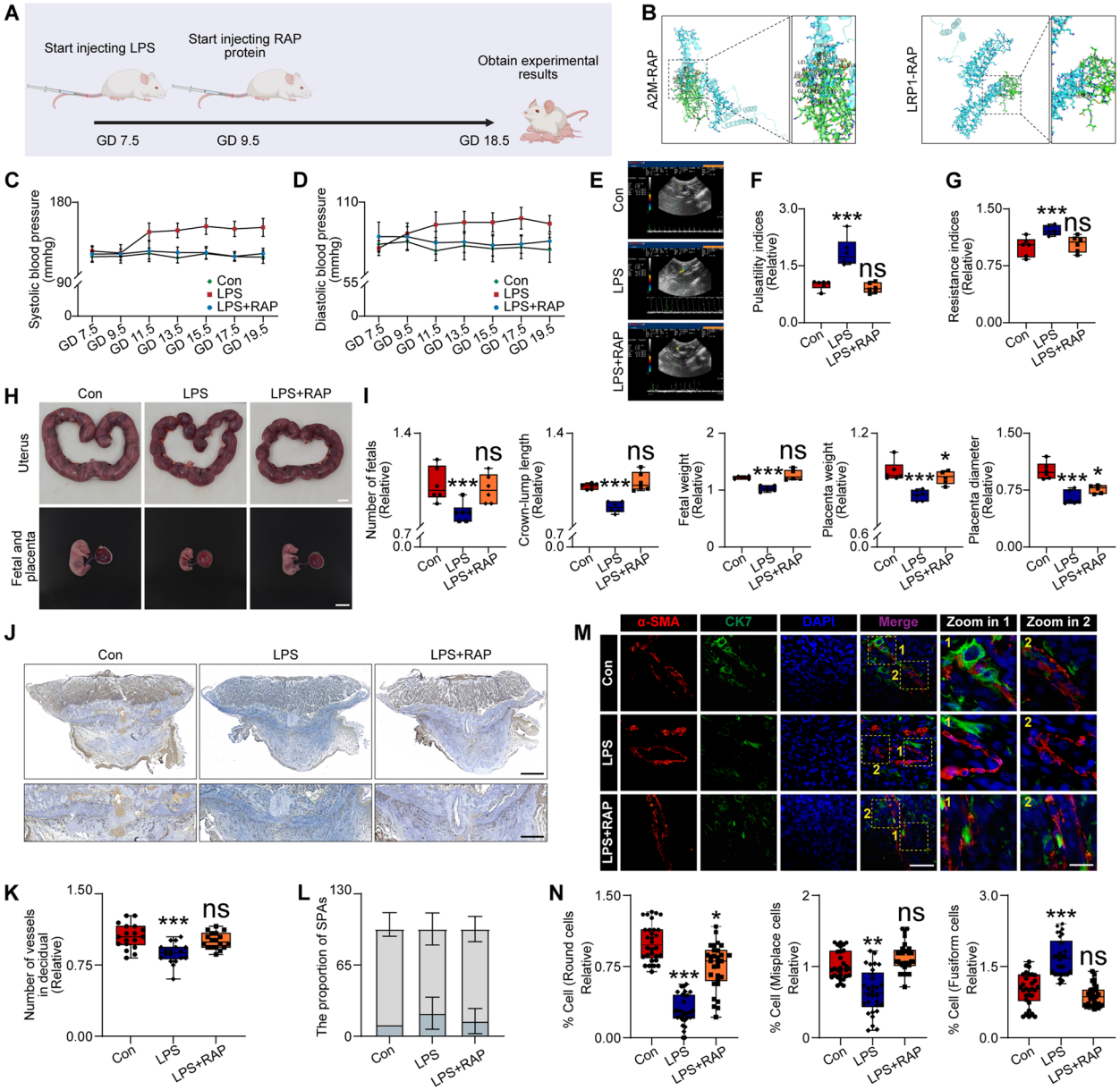

Fig. 9 Receptor-associated Protein (RAP) Ameliorates the pre-eclampsia phenotype in LPS-induced pre-eclampsia model rat. **A** Schematic diagram of the experimental. **B** Molecular docking of RAP, A2M, and LRP1. **C** Systolic and (**D**) diastolic blood pressure of pregnant rat.**E** Ultrasound evaluation showing that the uterine artery pulsatility index (**F**) and resistance index (**G**) were increased in the LPS group, while there was no significant difference between the RAP+LPS group and the control group. **H**, **I** Representative images of fetal rat and uterus (The scale bar is 1 cm, points in the graph representing the average of all fetal and appendage measurements delivered by each rat). **J** Representative images of immunohistochemistry of uterine spiral artery remodeling (Scale bar=300μm, the scale bar in the enlarged image is 150μm, three placenta-myometrium complexes randomly selected from each rat in each group, and 3 fields of view randomly selected for each complex for statistical analysis. Each point represents the observation of one placenta-myometrium complex, and the average of the results was calculated). **K**, **L** In the LPS group, the number and remodeling rate of blood vessels in the decidua and superficial muscle layer were reduced, whereas in the RAP+LPS group, these values were similar to those in the control group. **M**, **N** Representative immunofluorescence staining of rat decidual spiral artery α-SMA (red) and CK7 (green) showing that the roundness and displacement SMC rate in the LPS group were reduced, and the spindle SMC rate were increased (Scale bar=100μm, the scale bar in the enlarged image is 40μm, three random fields of view of 5 placenta-myometrium complexes selected from 6 rats in each group for observation, with each point in the statistical graph representing a placenta-myometrium complex and reflecting the average of the observations). Error bars, mean ± SD, with significance levels of * $P < 0.05$, ** $P < 0.01$, *** $P < 0.001$. A2M (α2-macroglobulin), LRP-1 (Low Density Lipoprotein Receptor-Related Protein 1), RAP (Receptor-associated protein), CK7 (Cytokeratin 7), α-SMA (α-smooth muscle actin), SMC (Smooth muscle cells), LPS (Lipopolysaccharide)

phenotype induced by LPS by influencing smooth muscle cell phenotypic switching and enhancing spiral artery remodeling.

Potential diagnostic and therapeutic implications of A2M for PE

Plasma A2M levels were significantly higher in early-onset pre-eclampsia and preterm pre-eclampsia during the third trimester (Fig. S7A-D). These levels were found to be a reliable predictor of delivery timing in pregnant women (Fig. S7E).

A2M displayed potential to identify preterm birth across different gestational age categories, with increased expression correlating with longer gestational ages (Fig. S7F). Time-dependent ROC analysis highlighted the potential of A2M to differentiate between extremely preterm, very preterm, moderately preterm, and late preterm infants, with AUC values ranging from 0.692 to 0.799 (Fig. S7G). Finally, a diagnostic model combining pre-eclampsia with preterm birth was developed by incorporating A2M characteristics into a generalized linear model. The specific fitting formula was $y=-42.864+0.134x$, and the Akaike information criterion (AIC) was 72.416 to evaluate the model's performance (Fig. S7H).

Discussion

Preeclampsia (PE) presents a persistent challenge in clinical management due to its complex and poorly understood pathophysiology. A hallmark of PE is the inadequate remodeling of spiral arteries (SPA-REM), a process that is critically dependent on the phenotypic switching of smooth muscle cells (SMC). This study identifies A2M as a key regulator that impairs SMC phenotypic switching by upregulating the RhoA GTPase pathway, which leads to cytoskeletal aggregation, reduced apoptosis, and insufficient vascular remodeling. Interestingly, receptor-associated protein (RAP) effectively counteracts the pathological effects of A2M by disrupting A2M-LRP1 interactions, thereby restoring SMC plasticity and promoting proper SPA-REM in a preeclampsia rat model. Moreover, elevated levels of A2M in PE patients were strongly correlated with disease severity, highlighting its potential as a biomarker for early diagnosis and as a tool for guiding personalized management strategies in high-risk pregnancies. These findings establish A2M as a central player in the pathogenesis of PE, offering valuable insights into its role as both a therapeutic target and a diagnostic marker. This dual utility could pave the way for innovative strategies aimed at mitigating the complications associated with PE, thereby enhancing our ability to address this complex pregnancy disorder.

To assess the role SMC phenotypic switching in uterine artery remodeling, morphological experimental results provide robust support for this hypothesis. Recent studies suggest that SMC loss during pregnancy is not permanent but represents a reversible process, facilitating vessel diameter expansion and the restoration of pre-pregnancy cellular characteristics postpartum [20, 31]. This dynamic reversibility underscores the importance of SMC phenotypic switching in vascular adaptation and offers promising avenues for therapeutic intervention in PE [32]. Using pseudo-time analysis, we further confirmed the synchronicity between A2M expression and SMC phenotypic switching, highlighting A2M as a potential therapeutic target for PE. However, our experiments revealed that decidual tissue secretions failed to counteract the inhibitory effects of A2M on SMC phenotypic switching. This limitation may be attributed to insufficient signaling molecules in the co-culture medium. Moreover, critical autocrine and paracrine regulatory mechanisms may be absent, further diminishing the restorative capacity of the medium. These findings suggest that the local microenvironment lacks sufficient compensatory signals to mitigate A2M's pathological effects, emphasizing the need for targeted therapeutic strategies.

Significant advances in SMC-based therapeutics, specifically in the area of cardiovascular disease [33]. Targeted regulation of SMC phenotype switching is one of the conceptual breakthroughs [34]. In addition to identifying molecular targets, selecting an efficient delivery method is crucial for optimizing smooth muscle cell therapy. Among the various delivery systems, adenoviral vectors present several advantages over nanoparticle and liposome-based systems. Their broad tropism, large gene capacity, and high transduction efficiency render them particularly valuable for gene therapy applications, including the development of oncolytic vectors and vaccine manufacturing [35–37]. Leveraging these properties, our study compared the therapeutic efficacy of two approaches targeting A2M in smooth muscle cells: knockdown tools delivered via adenoviral vectors and A2M-LRP1 receptor blockers. Our experimental results revealed that receptor blockers demonstrated superior efficiency compared to adenovirus-mediated knockdown tools. This disparity likely arises from the fundamental differences in their mechanisms of action. Receptor blockers exert their effects extracellularly, thereby bypassing the intracellular delivery, transcription, and translation processes required by adenoviral vectors. This direct action facilitates faster and more consistent results. Furthermore, receptor blockers possess chemically stable structures that are less susceptible to degradation or modification, thereby ensuring their functional integrity under experimental conditions [38]. In contrast, while

adenoviral vectors exhibit high transduction efficiency, their dependence on cellular uptake and subsequent intracellular mechanisms introduces potential variability. Factors such as varying rates of cellular uptake, immune responses, and the heterogeneity of target cells can diminish their effectiveness. Additionally, adenoviral vectors are vulnerable to host immune recognition, which may restrict their sustained action and complicate repeated administrations [39]. Our findings highlight the necessity of customizing therapeutic strategies to meet the specific needs of smooth muscle cell therapy. Receptor blockers present a robust option for acute interventions, providing rapid and stable modulation of signaling pathways.

LRP1, also known as the α2-macroglobulin receptor, is an endocytic receptor that mediates various physiological processes through ligand internalization [40]. Its interaction with A2M has been extensively studied in the context of conditions such as Alzheimer's disease and myocardial hypertrophy, highlighting its therapeutic potential [9, 10, 41, 42]. Recently, LRP1 has emerged as a target for cardiovascular diseases, with strategies including RAP antagonists or antibodies designed to inhibit A2M binding [9]. However, the specific role of A2M-LRP1 interactions in PE remains largely unexplored. Our findings revealed no significant differences in LRP1 expression in spiral artery SMC between PE patients and healthy controls. This observation aligns with the understanding that uterine spiral artery remodeling is a reversible and dynamic process. The absence of differential expression suggests that LRP1's role in PE may involve dynamic regulation of its activity or competitive ligand interactions to accommodate the transient nature of spiral artery remodeling. In a rat model, RAP administration significantly improved aberrant spiral artery remodeling and SMC phenotypic switching induced by LPS treatment, underscoring the critical role of A2M-LRP1 interactions in the pathogenesis of PE. Importantly, RAP treatment did not affect placental or fetal size, indicating a favorable safety profile. This safety may be attributed to RAP's biochemical properties as a 40–50 kDa protein, which likely prevents its crossing of the placental barrier, thereby minimizing fetal exposure [43, 44]. In conclusion, this study emphasizes the pivotal role of A2M-LRP1 interactions in spiral artery remodeling and the development of PE. These findings establish A2M-LRP1 as a promising therapeutic target and provide a foundation for future investigations into targeted therapies for PE and related placental disorders. Further mechanistic studies are necessary to validate these findings and explore their translational potential.

This study investigated the mechanisms through which A2M influences the phenotypic switching of SMC in PE, with a particular focus on its interaction with the RhoA-mDia signaling pathway. The RhoA family of GTPases is recognized for its role in the pathogenesis of PE by inhibiting trophoblast invasion and disrupting SMC regression, both of which are critical for the remodeling of uterine spiral arteries [23, 45, 46]. Dysregulation of these mechanisms is a hallmark of PE. Our findings demonstrated a consistent upregulation of A2M and key proteins associated with the RhoA-mDia pathway in decidual tissues, suggesting a synergistic regulatory interaction that aligns with existing evidence regarding their individual contributions to the progression of PE. A review of the literature yielded no studies specifically investigating the relationship between RhoA and A2M. To further investigate this relationship, we employed proteomics, molecular docking, LC-MS/MS analysis and immunoprecipitation analyses. These methods revealed a direct binding interaction between A2M and RhoA-associated proteins, providing novel insights into their regulatory roles. Mechanistically, A2M appears to modulate the phenotypic switching of SMC via the RhoA-mDia pathway, influencing cytoskeletal dynamics and the transition from a contractile to a synthetic phenotype, which is necessary for proper vascular remodeling. These findings enhance our understanding of the molecular underpinnings of PE and highlight the A2M-RhoA interactions as potential therapeutic targets. Future studies should further elucidate the downstream effects of this pathway and evaluate pharmacological strategies to modulate these interactions, thereby offering new avenues for improving maternal and fetal outcomes in PE.

Interestingly, the downregulation of RhoA GTPase observed in SMC following RAP treatment parallels the effects seen with A2M knockdown. This phenomenon likely relates to the role of LRP1 as an endocytic receptor that mediates ligand internalization and subsequent downstream signaling. By disrupting the A2M-LRP1 interaction, RAP may hinder the receptor's capacity to activate intracellular pathways, including RhoA GTPase signaling, which is crucial for cytoskeletal organization and SMC behavior. The endocytic nature of LRP1 may elucidate this effect, as receptor internalization typically regulates signal transduction by modulating the availability and activity of key ligands and their downstream effectors [47–49]. The observed decrease in RhoA GTPase activity indicates that RAP effectively obstructs the receptor-ligand interaction, thereby diminishing the signaling cascade necessary for maintaining the contractile phenotype of SMC. RAP's ability to modulate this interaction highlights its potential as a therapeutic agent for addressing SMC dysfunction, particularly in conditions such as preeclampsia, where abnormal phenotypic switching is a critical factor. Future studies should explore the broader implications

of RAP-mediated inhibition on LRP1-associated signaling networks to fully elucidate its therapeutic potential.

The timing of pregnancy termination is crucial in the management of late-gestation PE, particularly within the preterm window (34–37 weeks) and for full-term pregnancies. Delivery is the recommended intervention for severe cases of PE, as fetuses at these stages generally attain sufficient maturity to reduce risks for both mother and child [2]. Our findings indicate that elevated levels of A2M during hospitalization may serve as a potential biomarker for the risk of early preterm birth, offering a novel tool for optimizing delivery timing in the management of severe PE. Furthermore, the high expression of A2M in the decidual tissues of PE patients, particularly around inadequately remodeled spiral arteries, emphasizes its significance in the pathological diagnosis of PE. This localization suggests A2M's involvement in abnormal vascular remodeling, a hallmark of PE. Additionally, given that most women undergo multiple pregnancies and often exhibit consistent physiological patterns across them [1, 50], identifying A2M as a diagnostic marker presents opportunities for non-invasive strategies and pre-pregnancy preventive interventions. By harnessing A2M's diagnostic and prognostic potential, clinicians could develop personalized management plans for high-risk pregnancies. However, further research is necessary to validate the utility of A2M as a predictive biomarker.

This study highlights the role of A2M in the pathogenesis of PE, linking its elevated expression to abnormal SMC phenotypic switching and impaired remodeling of spiral arteries. Mechanistically, A2M regulates SMC behavior through the RhoA-mDia pathway, while RAP effectively mitigates these effects by blocking A2M-LRP1 interactions. This finding underscores the therapeutic potential of RAP in addressing SMC dysfunction. Furthermore, the expression level of A2M in the maternal circulation and its localization around inadequately remodeled spiral arteries suggest its potential as a biomarker for optimizing delivery timing and pre-pregnancy interventions. Future research should aim to validate the clinical applications of A2M and explore strategies targeting A2M-RhoA interactions to enhance outcomes in PE.

This study has several limitations. First, proteome sequencing was conducted on rat tissues instead of directly isolating smooth muscle cells. Subsequent cellular and mechanistic experiments confirmed the regulatory effects of A2M on the cytoskeleton and the RhoA-GTPase pathway, although species differences may exist. Second, this study primarily focused on the interaction between A2M and LRP1, without investigating the underlying reasons for the increase in endogenous A2M in cells or the alterations in LRP1 during the pathogenesis of PE. Finally, additional clinical trials are warranted.

Supplementary Information

The online version contains supplementary material available at https://doi.org/10.1186/s12964-025-02060-y.

Supplementary Material 1.

Supplementary Material 2.

Acknowledgements
The authors want to acknowledge the participants and investigators of Department of Obstetrics and Gynecology, The First Affiliated Hospital of Jinan University.

Authors' contributions
Zhengrui Huang performed most of the experiments and analyses, organized and wrote the first draft of the article. Ping Zhang provided proteomics sequencing experiments and analysis, Ruiping Chen, Lu Sun, Jingyun Wang, Zhengrui Huang, Jian Wang, Jiachun Wei, Wanchang Yin, Xinyao Lu, Yuzhen Ding participated in the collection of clinical samples, Xuesong Yang, Guang Wang, Ruiman Li Critically read the full text, provided guidance on ideas, and formatted and revised the images.

Funding
This work was supported by basic research project jointly funded by municipal schools (colleges) (Dengfeng Hospital), research on the mechanism and clinical diagnosis and treatment of ferroptosis in the occurrence of PE (No. 2023A03J1009), the Fundamental Research Funds for the Central Universities (No. 21624111). The funding agencies had no role in the design and conduct of the study; the collection, management, analysis, and interpretation of the data; or the preparation and approval of the manuscript.

Data availability
No datasets were generated or analysed during the current study.

Declarations

Ethics approval and consent to participate
This study received ethical approval from the Ethics Committee of the First Affiliated Hospital of Jinan University (ethical approval numbers: KY-2021-092 for blood collection and KY-2021-054 for decidua collection) and was conducted in strict accordance with the Declaration of Helsinki. The animal experiment was approved by the Animal Ethics Committee of Jinan University (approval number: 20210302-46).

Consent for publication
Not applicable.

Competing interests
The authors declare no competing interests.

Author details
[1]Department of Obstetrics and Gynecology, The First Affiliated Hospital of Jinan University, Guangzhou, China. [2]Department of Fetal Medicine, First Affiliated Hospital of Jinan University, Guangzhou, China. [3]Division of Histology and Embryology, Medical College, Jinan University, Guangzhou 510632, China. [4]International School, Guangzhou Huali College, Zengcheng, Guangzhou 511325, China. [5]Fifth Department of Medicine (Nephrology / Endocrinology / Rheumatology / Pneumology), University Medical Centre Mannheim, University of Heidelberg, Mannheim, Germany. [6]Department of Environmental & Occupational Health Sciences, University of Washington, Seattle, WA, USA. [7]Department of Obstetrics and Gynecology, Peking University Shenzhen Hospital, Shenzhen, China.

Received: 30 October 2024 Accepted: 20 January 2025
Published online: 24 February 2025

References

1. Overton E, Tobes D, Lee A. Preeclampsia diagnosis and management. Best Pract Res Clin Anaesthesiol. 2022;36(1):107–21.
2. Rana S, Lemoine E, Granger JP, Karumanchi SA. Preeclampsia: pathophysiology, challenges, and perspectives. Circ Res. 2019;124(7):1094–112.
3. Sakowicz A, Bralewska M, Rybak-Krzyszkowska M, Grzesiak M, Pietrucha T. New ideas for the prevention and treatment of preeclampsia and their molecular inspirations. Int J Mol Sci. 2023;24(15):12100.
4. Meggyes M, Miko E, Lajko A, Csiszar B, Sandor B, Matrai P, Tamas P, Szereday L. Involvement of the PD-1/PD-L1 co-inhibitory pathway in the pathogenesis of the inflammatory stage of early-onset Preeclampsia. Int J Mol Sci. 2019;20(3):583.
5. Zhang R, Jia L, Meng L, Peng H, Zhang D, He Q, Duan T, Wang K. PD-L1 enhances migration and invasion of trophoblasts by upregulating ARHGDIB via transcription factor PU.1. Cell Death Discov. 2022;8(1):395.
6. Hu XH, Li ZH, Muyayalo KP, Wang LL, Liu CY, Mor G, Liao AH. A newly intervention strategy in preeclampsia: targeting PD-1/Tim-3 signaling pathways to modulate the polarization of decidual macrophages. Faseb J. 2022;36(1):e22073.
7. Rehman AA, Ahsan H, Khan FH. α-2-Macroglobulin: a physiological guardian. J Cell Physiol. 2013;228(8):1665–75.
8. Vandooren J, Itoh Y. Alpha-2-Macroglobulin in inflammation, immunity and infections. Front Immunol. 2021;12: 803244.
9. Lagrange J, Lecompte T, Knopp T, Lacolley P, Regnault V. Alpha-2-macroglobulin in hemostasis and thrombosis: an underestimated old double-edged sword. J Thromb Haemost. 2022;20(4):806–15.
10. Lindner I, Hemdan NY, Buchold M, Huse K, Bigl M, Oerlecke I, Ricken A, Gaunitz F, Sack U, Naumann A, et al. Alpha2-macroglobulin inhibits the malignant properties of astrocytoma cells by impeding beta-catenin signaling. Cancer Res. 2010;70(1):277–87.
11. Wang J, Zhang P, Liu M, Huang Z, Yang X, Ding Y, Liu J, Cheng X, Xu S, He M, et al. Alpha-2-macroglobulin is involved in the occurrence of early-onset pre-eclampsia via its negative impact on uterine spiral artery remodeling and placental angiogenesis. BMC Med. 2023;21(1):90.
12. He Z, Wang G, Wu J, Tang Z, Luo M. The molecular mechanism of LRP1 in physiological vascular homeostasis and signal transduction pathways. Biomed Pharmacother. 2021;139:111667.
13. Chen J, Su Y, Pi S, Hu B, Mao L. The dual role of low-density lipoprotein receptor-related protein 1 in atherosclerosis. Front Cardiovasc Med. 2021;8: 682389.
14. Olbromski M, Mrozowska M, Piotrowska A, Kmiecik A, Smolarz B, Romanowicz H, Blasiak P, Maciejczyk A, Wojnar A, Dziegiel P. Prognostic significance of alpha-2-macrglobulin and low-density lipoprotein receptor-related protein-1 in various cancers. Am J Cancer Res. 2024;14(6):3036–58.
15. Lillis AP, Van Duyn LB, Murphy-Ullrich JE, Strickland DK. LDL receptor-related protein 1: unique tissue-specific functions revealed by selective gene knockout studies. Physiol Rev. 2008;88(3):887–918.
16. Kounnas MZ, Moir RD, Rebeck GW, Bush AI, Argraves WS, Tanzi RE, Hyman BT, Strickland DK. LDL receptor-related protein, a multifunctional ApoE receptor, binds secreted beta-amyloid precursor protein and mediates its degradation. Cell. 1995;82(2):331–40.
17. Bulmer JN, Innes BA, Levey J, Robson SC, Lash GE. The role of vascular smooth muscle cell apoptosis and migration during uterine spiral artery remodeling in normal human pregnancy. FASEB J. 2012;26(7):2975–85.
18. Liu W, Luo M, Zou L, Liu X, Wang R, Tao H, Wu D, Zhang W, Luo Q, Zhao Y. uNK cell-derived TGF-β1 regulates the long noncoding RNA MEG3 to control vascular smooth muscle cell migration and apoptosis in spiral artery remodeling. J Cell Biochem. 2019;120(9):15997–6007.
19. Whitley GS, Cartwright JE. Trophoblast-mediated spiral artery remodelling: a role for apoptosis. J Anat. 2009;215(1):21–6.
20. Ma Y, Yu X, Zhang L, Liu J, Shao X, Li Y-x, Wang Y-L. Uterine decidual niche modulates the progressive dedifferentiation of spiral artery vascular smooth muscle cells during human pregnancy†. Biol Reprod. 2021;104(3):624–37.
21. Frismantiene A, Philippova M, Erne P, Resink TJ. Smooth muscle cell-driven vascular diseases and molecular mechanisms of VSMC plasticity. Cell Signal. 2018;52:48–64.
22. Kim JG, Islam R, Cho JY, Jeong H, Cap KC, Park Y, Hossain AJ, Park JB. Regulation of RhoA GTPase and various transcription factors in the RhoA pathway. J Cell Physiol. 2018;233(9):6381–92.
23. Wu S, Cui Y, Zhao H, Xiao X, Gong L, Xu H, Zhou Q, Ma D, Li X. Trophoblast exosomal UCA1 induces endothelial injury through the PFN1-RhoA/ROCK pathway in preeclampsia: a human-specific adaptive pathogenic mechanism. Oxid Med Cell Longev. 2022;2022:2198923.
24. Xu J, Sivasubramaniyam T, Yinon Y, Tagliaferro A, Ray J, Nevo O, Post M, Caniggia I. Aberrant TGFβ signaling contributes to altered trophoblast differentiation in preeclampsia. Endocrinology. 2016;157(2):883–99.
25. Nugent WH, Mishra N, Strauss JF 3, Walsh SW. Matrix Metalloproteinase 1 causes Vasoconstriction and enhances Vessel reactivity to angiotensin II via protease-activated receptor 1. Reprod Sci. 2016;23(4):542–8.
26. Mishra N, Nugent WH, Mahavadi S, Walsh SW. Mechanisms of enhanced vascular reactivity in preeclampsia. Hypertension. 2011;58(5):867–73.
27. Gu Y, Feng Y, Yu J, Yuan H, Yin Y, Ding J, Zhao J, Xu Y, Xu J, Che H. Fasudil attenuates soluble fms-like tyrosine kinase-1 (sFlt-1)-induced hypertension in pregnant mice through RhoA/ROCK pathway. Oncotarget. 2017;8(61):104104–12.
28. Wu M, Liu W, Huang H, Chen Z, Chen Y, Zhong Y, Jin Z, Liu X, Zou L. PVT1/miR-145-5p/HK2 modulates vascular smooth muscle cells phenotype switch via glycolysis: the new perspective on the spiral artery remodeling. Placenta. 2022;130:25–33.
29. Zhang JY, Wu P, Chen D, Ning F, Lu Q, Qiu X, Hewison M, Tamblyn JA, Kilby MD, Lash GE. Vitamin D promotes trophoblast cell induced separation of vascular smooth muscle cells in vascular remodeling via induction of G-CSF. Front Cell Dev Biol. 2020;8:601043.
30. Wei P, Dong M, Bi Y, Chen S, Huang W, Li T, Liu B, Fu X, Yang Y. Identification and validation of a signature based on macrophage cell marker genes to predict recurrent miscarriage by integrated analysis of single-cell and bulk RNA-sequencing. Front Immunol. 2022;13: 1053819.
31. Staff AC. The two-stage placental model of preeclampsia: an update. J Reprod Immunol. 2019;134–135:1–10.
32. Liu Y, Du L, Gu S, Liang J, Huang M, Huang L, Lai S, Zhang S, Tu Z, Sun W, et al. Identification of the role of DAB2 and CXCL8 in uterine spiral artery remodeling in early-onset preeclampsia. Cell Mol Life Sci. 2024;81(1):180.
33. Liu M, Gomez D. Smooth muscle cell phenotypic diversity. Arterioscler Thromb Vasc Biol. 2019;39(9):1715–23.
34. Alexander MR, Owens GK. Epigenetic control of smooth muscle cell differentiation and phenotypic switching in vascular development and disease. Annu Rev Physiol. 2012;74:13–40.
35. Li X, Le Y, Zhang Z, Nian X, Liu B, Yang X. Viral Vector-based gene therapy. Int J Mol Sci. 2023;24(9):7736.
36. Muravyeva A, Smirnikhina S. Strategies for modifying Adenoviral vectors for Gene Therapy. Int J Mol Sci. 2024;25(22):7736.
37. Strecker MI, Wlotzka K, Strassheimer F, Roller B, Ludmirski G, König S, Röder J, Opitz C, Alekseeva T, Reul J, et al. AAV-mediated gene transfer of a checkpoint inhibitor in combination with HER2-targeted CAR-NK cells as experimental therapy for glioblastoma. Oncoimmunology. 2022;11(1): 2127508.
38. Ricobaraza A, Gonzalez-Aparicio M, Mora-Jimenez L, Lumbreras S, Hernandez-Alcoceba R. High-capacity adenoviral vectors: expanding the scope of Gene Therapy. Int J Mol Sci. 2020;21(10):3643.
39. Wallace R, Bliss CM, Parker AL. The Immune System-A double-edged Sword for Adenovirus-based therapies. Viruses. 2024;16(6):973.
40. Yamamoto K, Scilabra SD, Bonelli S, Jensen A, Scavenius C, Enghild JJ, Strickland DK. Novel insights into the multifaceted and tissue-specific roles of the endocytic receptor LRP1. J Biol Chem. 2024;300(8): 107521.
41. Guan PP, Yang LQ, Xu GB, Wang P. Indomethacin disrupts the formation of β-Amyloid plaques via an α2-Macroglobulin-activating lrp1-Dependent mechanism. Int J Mol Sci. 2021;22(15):8185.
42. Laberge A, Ayoub A, Arif S, Larochelle S, Garnier A, Moulin VJ. α-2-Macroglobulin induces the shedding of microvesicles from cutaneous wound myofibroblasts. J Cell Physiol. 2019;234(7):11369–79.
43. Knipp GT, Audus KL, Soares MJ. Nutrient transport across the placenta. Adv Drug Deliv Rev. 1999;38(1):41–58.
44. Simister NE. Placental transport of immunoglobulin G. Vaccine. 2003;21(24):3365–9.

45. Munchel S, Rohrback S, Randise-Hinchliff C, Kinnings S, Deshmukh S, Alla N, Tan C, Kia A, Greene G, Leety L, et al. Circulating transcripts in maternal blood reflect a molecular signature of early-onset preeclampsia. Sci Transl Med. 2020;12(550):eaaz0131.
46. Zhou L, Qiao F. Expression of RhoA in placenta of preeclampsia. J Huazhong Univ Sci Technolog Med Sci. 2006;26(6):744–6.
47. Prasad JM, Migliorini M, Galisteo R, Strickland DK. Generation of a potent low density lipoprotein receptor-related protein 1 (LRP1) antagonist by Engineering a stable form of the receptor-associated protein (RAP) D3 domain. J Biol Chem. 2015;290(28):17262–8.
48. Shinohara M, Tachibana M, Kanekiyo T, Bu G. Role of LRP1 in the pathogenesis of Alzheimer's disease: evidence from clinical and preclinical studies. J Lipid Res. 2017;58(7):1267–81.
49. Sizova O, John LS, Ma Q, Molldrem JJ. Multi-faceted role of LRP1 in the immune system. Front Immunol. 2023;14: 1166189.
50. Okoth K, Chandan JS, Marshall T, Thangaratinam S, Thomas GN, Nirantharakumar K, Adderley NJ. Association between the reproductive health of young women and cardiovascular disease in later life: umbrella review. BMJ. 2020;371:m3502.

Publisher's Note